Application of Segmented 2-D Probabilistic Occupancy Maps for Robot Sensing and Navigation

Bassel Abou Merhy, Pierre Payeur, *Member, IEEE*, and Emil M. Petriu, *Fellow, IEEE*

Abstract—The concept of probabilistic occupancy maps was introduced by the end of the 1980s. Over the years, research has focused on the definition of the representation, the data fusion, and the generation of such occupancy models. However, few considerations have been given to processing occupancy maps as textured images to extract meaningful information that is required for robot navigation. This paper investigates the application of modern segmentation techniques over 2-D probabilistic occupancy maps that are encoded as textured images. Enhancements are proposed to a uniformity estimation technique based on local binary pattern and contrast (LBP/C) to achieve the robust segmentation of occupancy maps that typically result from range sensors with limited resolution. The enhanced LBP/C segmentation technique handles occupancy uncertainty and subdivides the space in regions that are characterized by three deterministic occupancy states, which are defined as free, unknown, and occupied. The approach is also extended to increase the number of classification levels, which provides the necessary flexibility to automatically select the regions that are characterized by a given range of occupancy states. The use of these extensions, along with the accuracy of the segmented 2-D occupancy maps, is first experimentally demonstrated on ground-based probabilistic grids for application in mobile robot navigation with collision avoidance. The potential of the proposed approach is also evaluated on aerial and satellite images for which it provides stable results and can find applications for unmanned aerial vehicle navigation.

Index Terms—Local binary pattern, mobile robot navigation, probabilistic maps, texture segmentation, unmanned aerial vehicles (UAVs).

I. INTRODUCTION

OCCUPANCY maps have long been proposed as a compact representation of space occupancy. Navigating mobile robots from such maps permitted the development of efficient robotic platforms while keeping the amount of processing at a relatively low level. However, most occupancy maps discussed in the literature assume perfectly reliable knowledge about the state of the robot workspace, which results in deterministic maps where regions are either empty, occupied, or have not been explored. Applying these types of maps for

safe robot navigation with autonomous perception capabilities implies that the regions are scanned without any gap between the viewpoints and that sensors are perfectly calibrated. Elfes [1] evolved this representation with the inclusion of uncertainty using a Bayesian merge technique to combine uncertain range measurements that are collected from several viewpoints. The resulting probabilistic occupancy maps represent a bidimensional mosaic in which every cell is tagged with an estimate OP of the probability that the cell is actually occupied, where $OP \in [0, 1]$. Such occupancy maps can be readily encoded as textured images, where low OP values represent areas that are most certainly empty, and high OP values correspond to regions where obstacles are most certainly present.

The use of probabilistic occupancy maps alleviates the constraints that are imposed by deterministic occupancy maps as uncertainty is directly encoded into the maps. On the other hand, the identification of secure areas for the mobile robot to circulate is made more difficult as maps no longer show uniformity and sharp transitions. Instead, intermediate regions between free passages and obstacle boundaries exhibit progressive variations of the OP values. As a result, probabilistic occupancy maps are characterized by the fuzziness of the texture distribution, which makes the segmentation and the identification of free paths a challenging task. In spite of a wide interest in this type of mapping, complications still arise from the fact that existing segmentation methods are extremely specialized and generally address only one preset type of image.

Typically, segmentation algorithms try to classify the pixels of an image based on their intensity or color properties and on their spatial relationship with their entourage. Thereafter, the goal of the segmentation is to divide an image into areas that are characterized by homogeneous properties. Several segmentation approaches have been proposed in the literature that can be classified either as region based, boundary based, or a combination of the two. In addition, segmentation is either supervised or unsupervised. Unsupervised segmentation is applied in cases where no *a priori* information about the contents or the textures of the image is available, as found in the context of robot navigation and exploration. Approaches based on classical methods, such as split and merge [2], pyramid node linking [3], [4], as well as quadtrees [5] for the combination of statistical and spatial data, were the first to provide unsupervised region-based segmentation. Recent unsupervised segmentation methods explore, on one hand, multiresolution filtering using Gabor filters [6]–[8] or wavelets [9], [10] and, on the other hand, statistics with hidden Markov fields [11], [12]. This paper, which is an extended version of [13], refines, adapts, and tests an innovative segmentation approach to operate on

occupancy maps that contain uncertainty, as obtained from a mobile range finder with a limited field of view and resolution. Beyond the work described in [13], the framework is expanded to multilevel segmentation that is capable of creating uniform clusters of occupancy probability over variable ranges. It also evaluates the technique on different types of occupancy maps, as obtained from aerial and satellite images.

In the specific context of autonomous mobile robotic exploration, the value OP, which is associated with each cell of the occupancy map, corresponds to the probability of this cell being occupied. This information is mapped as a clustered distribution of textures, where the gray scale is made proportional to the local OP value in a given region. As a result, probabilistic occupancy maps are advantageously encoded as grayscale images to facilitate their manipulation. Therefore, region-based segmentation appears to be well suited to ensure obstacle location and identification of safe areas for the robot to navigate. In addition, object identification can eventually be achieved by shape recognition of those clusters to provide controlled interaction with the environment. Considering that the workspace configuration is initially unknown and gets scanned by a laser range finder only along specific directions, the resulting map of the explored space is characterized by a series of edges corresponding to the rays that are emitted by the active range sensor. Under such conditions, a segmentation approach that combines contrast and texture properties to identify regions of uniform density is revealed to be an appropriate strategy for differentiating between segments that are present in the probabilistic map.

These considerations motivated the exploration of Ojala *et al.*'s segmentation technique [14]–[16] that is based on "local binary pattern" and "contrast" (LBP/C) metrics to subdivide images with sharp patterns. However, unlike the images that they considered, in probabilistic maps, transitions between free and occupied spaces do not define such clear boundaries. The latter are rather spread out according to the uncertainty level that is introduced by the sensor model. In this paper, the original LBP/C segmentation mechanism is revisited to handle smooth transitions in complex images while achieving accurate contour definition. An evaluation is conducted on the application of such segmented probabilistic occupancy maps for path planning and collision avoidance with a mobile robot and for unmanned aerial vehicle (UAV) navigation from aerial or satellite images. For the navigation to be successful, the probabilistic space must first be segmented into areas of a relatively large size with a uniform occupancy state for the vehicle to choose whether a given region can be safely navigated. As a consequence, the success of the path-planning operation extensively depends on the success of the probabilistic occupancy map segmentation. This aspect has not been widely investigated in the literature while taking into account realistic sensing mechanisms that do not provide absolute knowledge about the state of the space and, therefore, lead to maps with uncertainty.

The following sections summarize the revisited probabilistic map-segmentation technique based on the double distribution of LBP/C, which is used to describe textures, as inspired by Ojala *et al*. Next, some extensions of the proposed segmentation technique are investigated to demonstrate the potential of the approach for the application with various types of mobile robots, including unmanned aerial robot navigation.

II. ENHANCED SEGMENTATION ALGORITHM

In a similar way to the approach introduced by Ojala and Pietikäinen [14], the proposed segmentation algorithm is divided into three phases, i.e., the hierarchical division, the segment creation, and the refinement step. The first phase of the proposed method is similar to that of the original algorithm. However, the proposed approach introduces major changes into the second and third stages to adapt and optimize the original algorithm to handle probabilistic images while significantly reducing the computation time.

The first phase divides the image into areas that are characterized by roughly uniform textures. Thereafter, the segment-creation step combines similar adjacent regions into segments that only approximate the various regions that are present in the image. Last, a refinement stage is applied to increase the accuracy on contour localization.

A. Hierarchical Division

This phase hierarchically subdivides the original image into square blocks of variable sizes but of relatively uniform textures. A new uniformity test is introduced to determine if a given region of size $[\alpha \times \alpha]$ contains heterogeneous textures associated with different occupancy states that therefore, must be subsequently subdivided into four subregions of equal size. Initially, the four subregions of size $[(\alpha/2) \times (\alpha/2)]$ are identified, and a logarithmic likelihood ratio is computed between each of the six possible pairs.

The logarithmic likelihood ratio developed by Sokal and Rohlf [17] can verify the validity of the correspondence between two probabilistic distributions. This statistical test advantageously compares to other statistical methods, such as the chi-square and the Kolmogorov–Smirnov distribution tests [18]. Beyond its relatively fast execution, one main advantage is its additive nature, which is beneficial for segmentation and merge techniques, where the values of different clusters can be easily combined. Sokal and Rohlf [17] define the logarithmic likelihood ratio, or G-statistics, as follows:

$$
\begin{aligned}
G^{\alpha/2} = {} & 2\left[\sum_{s,m}\sum_{i=1}^{n} f_i \times \log(f_i)\right] \\
& - 2\left[\sum_{s,m}\left(\sum_{i=1}^{n} f_i\right) \times \log\left(\sum_{i=1}^{n} f_i\right)\right] \\
& - 2\left[\sum_{i=1}^{n}\left(\sum_{s,m} f_i\right) \times \log\left(\sum_{s,m} f_i\right)\right] \\
& + 2\left[\left(\sum_{s,m}\sum_{i=1}^{n} f_i\right) \times \log\left(\sum_{s,m}\sum_{i=1}^{n} f_i\right)\right] \quad (1)
\end{aligned}
$$

where f_i corresponds to the number of pixels that are characterized by a pair of LBP/C values in bin i. s and m represent

the two distributions to compare, and n is the number of bins in each of them. Among the six possible pairs of subregions resulting from the subdivision described earlier, the ones with the largest and smallest G-statistic values, respectively denoted by $G_{\max}^{\alpha/2}$ and $G_{\min}^{\alpha/2}$, are identified.

The uniformity between blocks is evaluated with a uniformity test, which is defined as follows:

$$R^\alpha = \frac{G_{\max}^{\alpha/2}}{G_{\min}^{\alpha/2}} > X, \quad \alpha \in \{64, 32, 16\}. \tag{2}$$

The parent block is considered nonuniform and, thus, subdivided if the ratio between $G_{\max}^{\alpha/2}$ and $G_{\min}^{\alpha/2}$ is larger than a certain threshold, which is designated by X. The values of α in (2) correspond to the possible sizes, in pixels, of the regions that successively undergo the uniformity test, if needed. Details about the manipulation of blocks of different sizes over the probabilistic map during the hierarchical division phase are discussed in [13]. On the other hand, the setting of the threshold value X is guided by the fact that supplementary subdivisions between regions without strong distinctive features can easily be corrected in the second phase. On the contrary, segments that are missed in the first phase cannot be reintroduced afterward. An oversegmentation is, therefore, privileged in this early phase, which implies a relatively low value for the uniformity ratio threshold. In the case of 2-D probabilistic maps, a value of $X = 1.2$ was experimentally obtained and considered to perform well since 20% of variation between the largest and smallest G-statistic values corresponds to a perceptible deviation between the region textures.

B. Segment Creation

This phase merges similar neighboring regions until a convergence criterion is met. Fusion between adjacent blocks is performed when an average occupancy probability OP_i for each block is in the same range. This parameter represents the average pixel intensity level I in a region R_i of size $[N \times M]$ and is determined as follows:

$$OP_i = \frac{1}{M \cdot N} \sum_{k=0}^{M-1} \sum_{l=0}^{N-1} I(r_{k,l}) \Big| r_{k,l} \in R_i. \tag{3}$$

The choice of the OP parameter to evaluate the texture similarity between adjacent regions is related to the structure of the probabilistic occupancy map in which pixel intensity values correspond to the probability of the space occupancy. After normalizing the pixels' values over the range [0, 1], if a region is totally unknown, it is characterized by an OP of 0.5; if the region is scanned by a range sensor, two possibilities exist—either it generates an OP value below 0.5, and this corresponds to the case where the region of the space is mostly free, or it produces an OP value that is higher than 0.5, which involves a mostly occupied region of the space.

For the purpose of safe robot navigation, the probabilistic map usually needs to be segmented into regions that are characterized by deterministic states S, i.e., $S(R_i) \in$ {free, unknown, occupied}, upon which navigation decisions
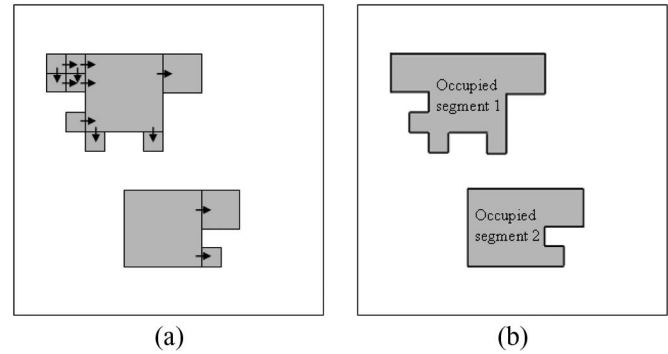

(a) (b)

Fig. 1. Construction of disconnected occupied segments during the segment creation phase using a search for downward and right-hand side neighbors.

can be performed. These states, respectively, fall into the following ranges of OP values—[0, 0.498], [0.498, 0.502], and [0.502, 1]. We chose to have a small tolerance over the interval relative to the unknown state, i.e., 0.5, to ensure that the regions that are mainly unknown but have very few free or occupied cells are classified in accordance with the state of the predominant cells. This consideration reduces the number of pixels to be reclassified during the refinement phase. Following this evaluation, the segment creation process starts by merging the subdivisions whose OPs are limited within the intervals [0, 0.498] and [0.498, 0.502] to build the free and unknown segments, respectively. At the end of this process, only the subdivisions that are considered occupied are not classified. The construction of the occupied segments requires a traversal of the unclassified subdivisions as many times as there are nonadjacent objects in the environment. For every iteration, the first unclassified subdivision that is met is regarded as being a distinct occupied segment. Thereafter, the algorithm carries out the identification of its occupied neighbors on the right and down sides. Each time such a subdivision is met, it is merged with the segment in the course of construction. The process iteratively continues until no addition to the current occupied segment is possible. The fact of considering nonadjacent occupied areas as separate entities avoids any possible confusion in the recognition of objects and the interaction of an autonomous robot system with its environment. Fig. 1 illustrates the construction of the occupied segments from adjacent subdivisions that are characterized by an OP in the interval [0.502;1]. This shows how the algorithm automatically constructs segments of uniform occupancy by searching for each subdivision among its occupied neighbors on the right-hand and downward sides, allowing for separate objects to be recognized as different entities, in spite of the fact that they share occupancy state values in the same interval.

One of the major problems encountered with the original algorithm proposed in [14] when applied on probabilistic maps comes from the fact that it does not succeed in correctly merging segments that correspond to a known space that is either free or occupied. Thereafter, Ojala *et al.*'s algorithm cannot identify the occupied and free spaces as unique segments. In addition, this algorithm is not meant to provide any information about the occupancy state of the segmented regions. For these reasons, applications such as path planning for autonomous mobile
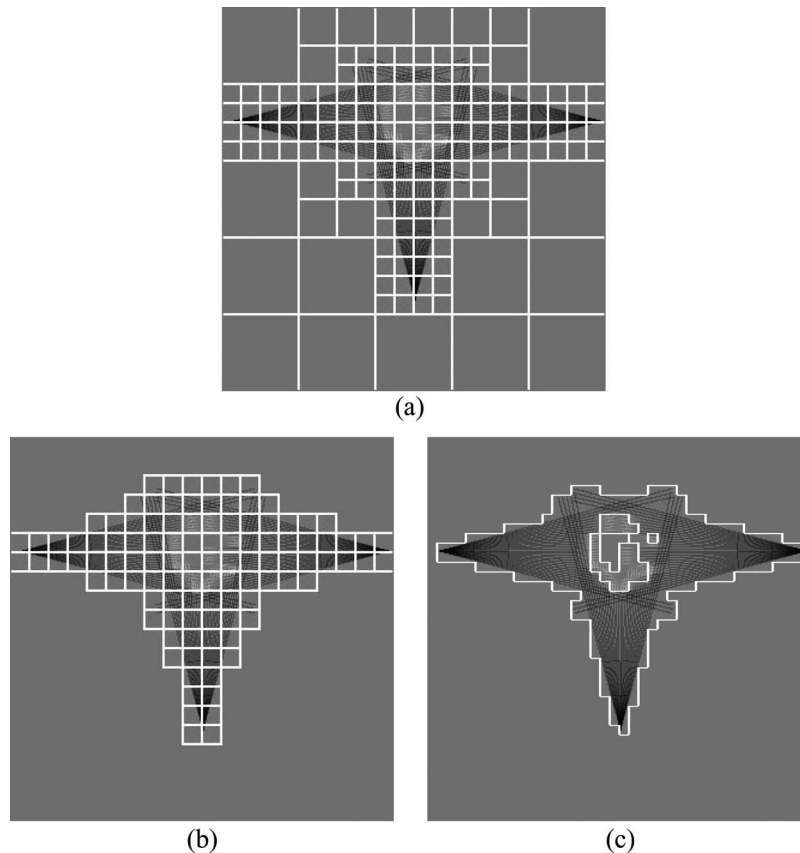
Fig. 2. Comparison between the segments obtained from (a) initial hierarchically subdivided probabilistic map using (b) original LBP/C algorithm and (c) proposed enhanced approach.

robots cannot rely on the original LBP/C algorithm [14] as is. Fig. 2 provides a comparison between the segmentation results that are obtained on the same probabilistic map with the algorithm proposed in [14] and with the enhanced approach presented here after the merging phase. This shows that the original LBP/C algorithm fails at properly merging adjacent uniform regions into single segments over regions that are partially empty and partially occupied, whereas the improved segmentation approach successfully groups free and occupied regions of the space in distinct but unified regions that are optimal for robot navigation. In Fig. 2, dark cells represent an empty space, light cells map an occupied space, and medium grayscale cells correspond to unknown or unexplored areas. White lines define the contours of detected uniform segments. This example also illustrates the major segmentation improvement that is achieved by means of the enhanced segment creation phase [Fig. 2(c)] over the initial hierarchical subdivision [Fig. 2(a)], as distinct regions of the workspace are already individually clustered.

C. Refinement

Last, segmentation results are refined by reclassifying the pixels that are located on the edges between two adjacent regions. The refinement step is based on the fact that the range of OP values leading to an unknown segment classification is narrow, being limited to the interval [0.498, 0.502]. Even if a segment overlaps between an unknown space and a known one (free or occupied) by a limited number of pixels, it will still

be considered to be known by the segment creation phase. As a consequence, the space whose occupancy is known always juts out into the unknown one, which represents potentially hazardous situations for safe robot navigation.

A process of compaction must be applied to the free and occupied segments to better delimit them and to expand unknown segments where necessary. At the implementation level, this process consists of scanning the probabilistic image along each of the four possible horizontal and vertical directions: right–left, left–right, down–up, and up–down. For each of the scans, when a boundary between an unknown and a known space is found, pixels of the known space that have a value of 0.5 are reclassified as belonging to the unknown region until a pixel with a different value is met. The four-direction scanning procedure ensures the coverage of all possible boundary shapes.

The refinement step implements this compaction process between the free/occupied segments and the unknown segments that are adjacent to them. Since free and occupied spaces do not define clear boundaries in probabilistic maps given that the sensor's uncertainty is taken into account, the compaction process is revisited. Boundaries between free/occupied (occupied/free) spaces are scanned as for the compaction process previously described, from the four possible sides; however, in this case, if a pixel on the boundary has an occupancy probability that is equal to or lower than (equal to or higher than) 0.5, three successive pixels are considered along the scanning direction. Three cases are then possible. First, if the three pixels have a value of 0.5, no reclassification is done; this case ensures that
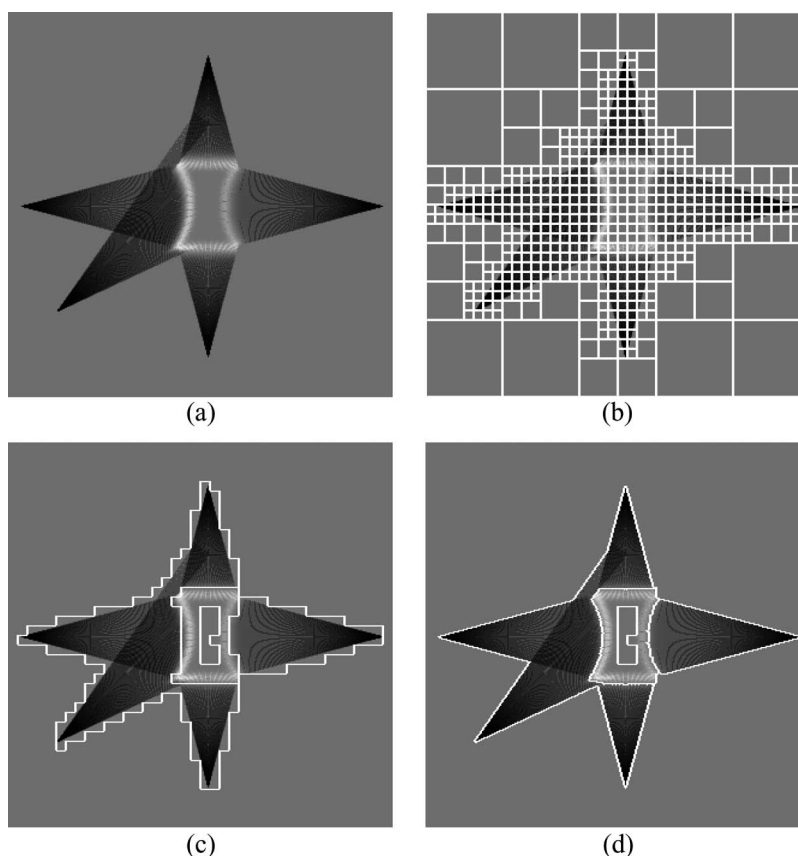
Fig. 3. Probabilistic map segmentation on a concave object. (a) Initial probabilistic map. (b) Hierarchical subdivision. (c) Segment creation. (d) Refinement phase.

no holes are created in the segments due to the fact that the rays emitted by the range sensor do not cover the entire space and are often separated by unknown cells due to the angular resolution of the sensor. Second, if at least one of the pixels has an occupancy probability that is strictly lower (higher) than 0.5, the pixels, up to the one under observation, are reclassified as being free (occupied). The third case corresponds to the situation in which no classification occurs due to the fact that an occupied (free) cell is encountered.

The enhanced LBP/C segmentation has been applied on various probabilistic maps representing cluttered bidimensional workspaces. In the cases reported here, the evaluation of performance was conducted on objects featuring curved surfaces to ensure that the proposed technique, which relies on the manipulation of a map of square cells, would properly handle situations where obstacles exhibit free shapes. The first map [Fig. 3(a)] contains an object resembling a divergent lens, whereas the object used in the second map [Fig. 4(a)] is made of two collateral circles. Both probabilistic maps are of size [320 × 320] pixels. They have been generated using a mobile laser range finder simulator for 2-D surface mapping that was developed in previous work [19]. The number and positions of the range sensor's points of view differ between maps. In Figs. 3(a) and 4(a), white pixels represent the surface of the objects, dark pixels correspond to the free space, and intermediate grayscale pixels map unexplored areas. In the case of Fig. 3(a), five range sensor scans are taken with a Gaussian

standard deviation ($\sigma = 5$ cm) on the range measurements that cover up to a 2-m distance. These scans are merged to build the probabilistic map. In Fig. 4(a), eight scans with a Gaussian standard deviation ($\sigma = 3$ cm) are used. The step angle between two adjacent sensor's rays, which defines the angular resolution, is fixed to $0.5°$ in all maps to create nonuniform textures in explored spaces.

The parameters used for the implementation of the segmentation technique are the same as the ones described in the preceding sections. In the hierarchical division phase, the size of the first level of subdivided blocks is [64 × 64] cells, and three subdivision levels are conducted, leading to a minimum subdivision level of [8 × 8] cells. Figs. 3(b) and 4(b) present the results of the hierarchical division phase of the algorithm, whereas Figs. 3(c) and 4(c) show the segmented maps after the segment creation phase. The segments obtained at the end of the second phase already approximate well the shape of the regions that are present in the probabilistic images; nevertheless, the rough localization of contours between the free and unknown spaces is obvious in Figs. 3(c) and 4(c).

Segmentation results obtained after the refinement phase are shown in Figs. 3(d) and 4(d) for the two probabilistic maps, respectively. Important improvement on contour definition around the objects and the boundaries of the explored space is achieved. The boundary between occupied and unknown cells that are located inside the objects is not refined in the third phase because this area is dominated by uncertainty as it is
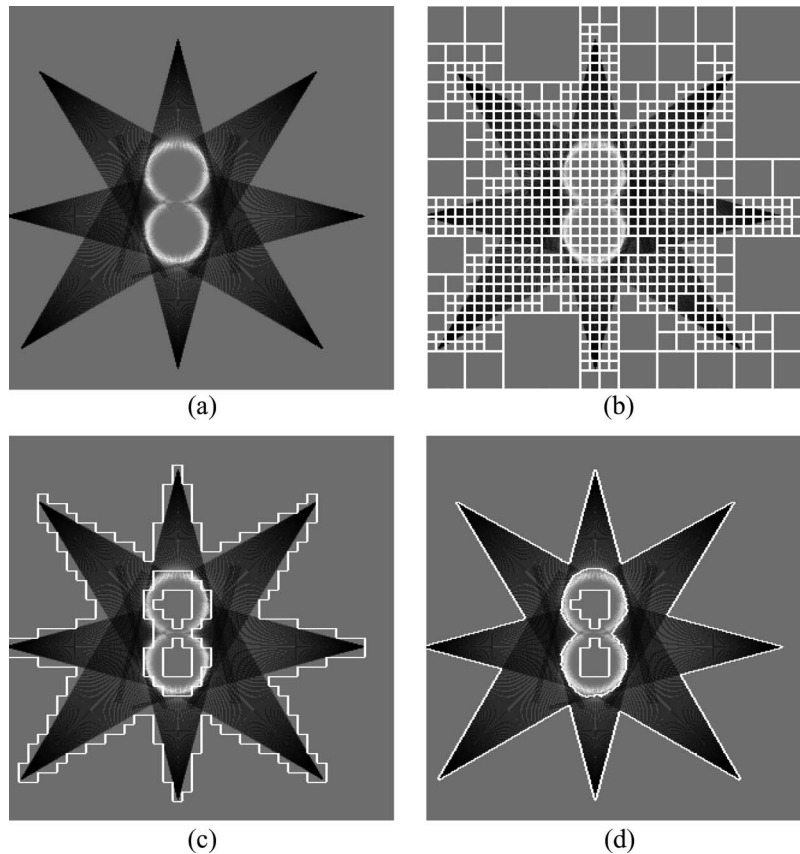
Fig. 4. Probabilistic map segmentation with extra viewpoints. (a) Initial probabilistic map. (b) Hierarchical subdivision. (c) Segment creation. (d) Refinement phase.

occluded from any scan by the object surface. However, these regions cannot be navigated by a robot as they represent the interior part of objects.

III. SEGMENTATION ALGORITHM EXTENSIONS AND APPLICATIONS

Building upon the stability of the proposed technique, this section investigates various extensions and applications of the enhanced LBP/C segmentation algorithm. The first one divides the global OP range [0, 1] into intervals of the same width that is specified by the user and merges in segments all adjacent subdivisions that have an OP within a given range of values. The second extension allows the extraction, from a probabilistic image, of the segments whose OP value falls within a specific interval that is defined by the user, which leads to an immediate application in mobile robot path planning. Last, the proposed segmentation scheme is validated on slightly different models of the environment, i.e., aerial and satellite images, as found in UAV navigation.

A. Segmentation by Levels of OP Values

In the original context of robotic systems navigating without collisions reported in [13], the proposed algorithm identifies as specific segments only those regions in which the occupancy probability OP belongs to three distinct intervals, associated with *free*, *unknown*, and *occupied* spaces, respectively.

To evaluate the generality of the segmentation approach, we reformulated the segment creation phase, so that it merges adjacent subdivisions whose OP values fall in a larger set of intervals, such that more features that are characterized by distinct intensities can be identified. This opens a wide range of applications in pattern recognition from maps within which several objects or regions can appear while being characterized by different texture characteristics.

Considering that the chosen interval's width is P, the first segment merges adjacent regions whose OP values are bounded within $[0, P]$. The second segment is composed of regions with OP values within $[P, 2P]$, the third segment is bounded within $[2P, 3P]$, and so on, until the highest boundary of the nth interval $nP \geq \max(OP)$. In practice, the probabilistic maps considered are normalized over the interval [0, 1]; therefore, the entire occupancy map is segmented into up to n regions according to the probabilistic distribution of occupancy.

Figs. 5 and 6 show the results of such segmentation by levels of OP values on two probabilistic images with interval width P of 0.1 and 0.15, respectively. The first part of these figures [Figs. 5(a) and 6(a)] corresponds to the probabilistic map encoded as a grayscale image, whereas the second part [Figs. 5(b) and 6(b)] represents the segmentation results after the segment creation phase. The intensity of the segments in the third part [Figs. 5(c) and 6(c)] is uniformly colored according to the interval of OP values, which characterizes each of them. The higher the range of OP values of a specific segment, the clearer the grayscale level in the final representation. We notice
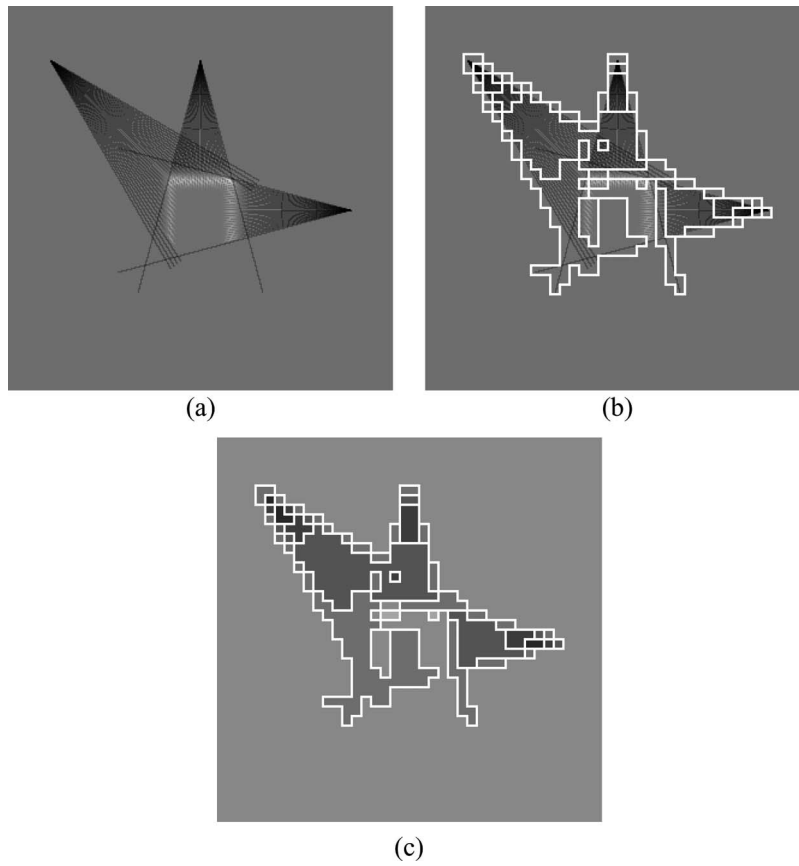
Fig. 5.   Segmentation by levels of occupancy probability values with an interval width of 0.1 [each gray level in (c) represents a specific interval].
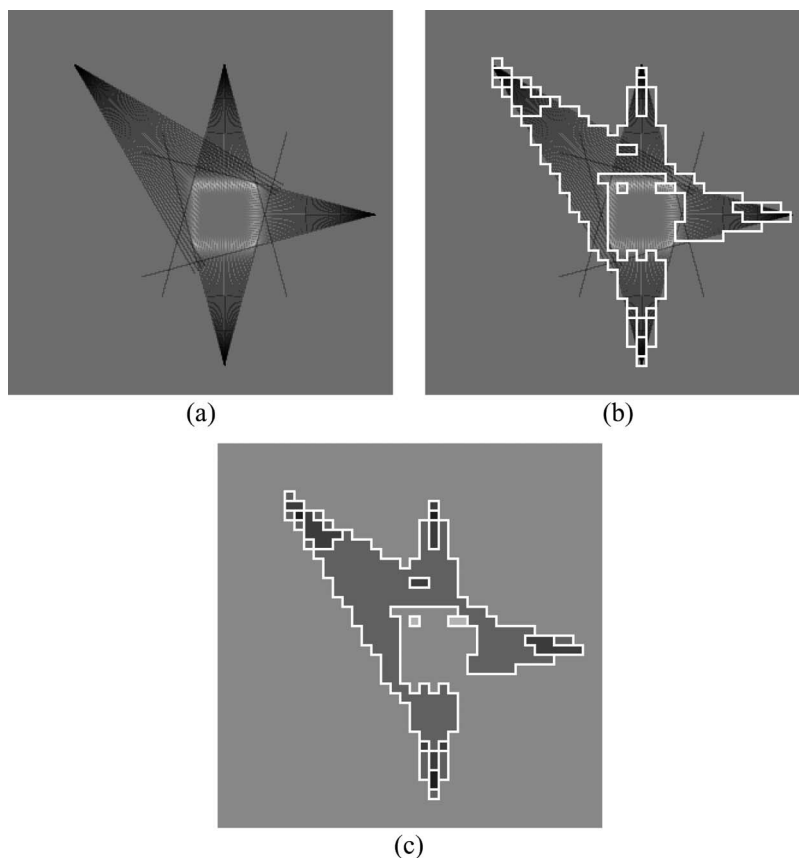

Fig. 6.   Segmentation by levels of occupancy probability values with an interval width of 0.15 [each gray level in (c) represents a specific interval].
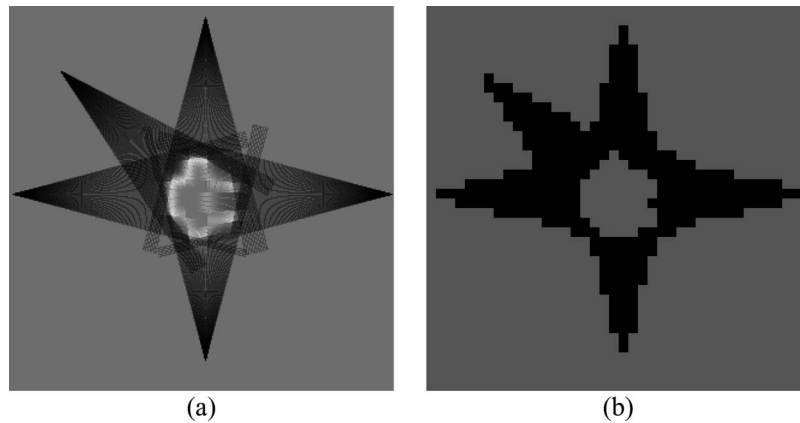
Fig. 7. Extraction of the region whose occupancy probability is bounded within the interval [0, 0.35]. (a) Original probabilistic map. (b) Segmented region in black belonging to the interval of interest (empty space).
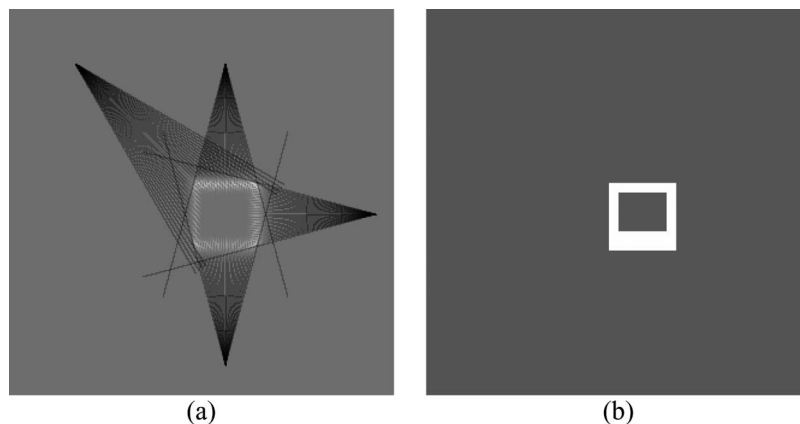

Fig. 8. Extraction of the region whose occupancy probability is bounded within the interval [0.52, 0.7]. (a) Original probabilistic map. (b) Segmented region in white belonging to the interval of interest (occupied space).

that in the free space [dark in the original occupancy maps of Figs. 5(a) and 6(a)], the OP value becomes increasingly high (pixels are becoming clearer) when one moves away from the sensor, i.e., from the vertex of the triangular area in the map. This is due to the fact that with the distance from the sensor, the confidence in the occupancy state decreases as the laser scans become sparser because of the limited angular resolution of the range sensor.

By comparing Figs. 5(c) and 6(c), we notice that the wider the segmentation intervals P, fewer the uniform segments will be generated, as expected, due to the reduction of the number of intervals of OP values considered and, consequently, the number of possible segments. However, the segmentation remains robust to the sparse distribution of scans over the surface and to the progressive variation of occupancy state values.

B. Extraction of Regions Within a Specific Occupancy Range

The second extension builds upon the previous one and introduces the capability to combine in connected segments some adjacent regions whose OP value falls within a specific interval that is chosen by the user. In this case, only segments that are characterized by the selected range of occupancy probability are highlighted by the segmentation procedure and connected together as much as a physical interconnection is

possible, given their respective spatial distribution. In addition to being relevant for the segmentation of grayscale images, this extension is particularly useful in applications of path planning and interaction with the environment in which the movements of a robot can only be limited to certain areas that are characterized by a specific occupancy state, e.g., an obstacle-free space.

Under this scheme, if two nonadjacent regions are characterized by an OP in the chosen interval but are not physically connected, each one of them will be automatically classified as a distinct segment. This functionality provides a direct input for path planning that can easily recognize if a path exists between a departure and a destination point, regardless of whether both are located in adjacent free areas or not.

Figs. 7 and 8 show two probabilistic images created from five and four sensor viewpoints, respectively, and the resulting segments for two different occupancy probability intervals, [0, 0.35] and [0.52, 0.7], respectively. These results demonstrate the use of the extension that allows the direct extraction of the regions that are characterized by a specific occupancy state in spite of strong texture variations around the objects' boundaries originating from a sparse scan of the environment and from the level of uncertainty on range measurements. The environment space that is not included in the chosen interval is shown in the intermediate gray level, whereas the identified segments are
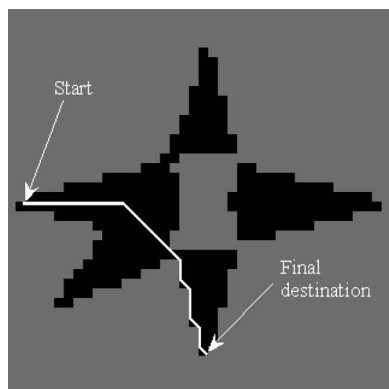
Fig. 9. Trajectory obtained with the A^* path planning restricted to the safe travel space (black cells) identified from a segmented map over the interval of the occupancy probability [0, 0.45].

Fig. 10. Trajectory obtained with the A^* path planning restricted to the safe travel space (black cells) identified from a segmented map over the interval of the occupancy probability [0, 0.45].
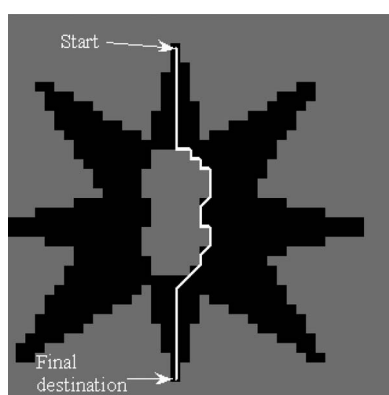
characterized by black pixels for the empty space [Fig. 7(b)] or white pixels for the occupied space [Fig. 8(b)].

C. Mobile Robot Path Planning

The enhanced LBP/C segmentation technique has been tested as a preliminary processing stage for path planning from probabilistic occupancy maps with a standard A^* path-planning algorithm [20]. The A^* algorithm guides a mobile robot by successive minimization of the remaining Euclidean distance to the destination position while avoiding prohibited areas. For testing purposes, safe travel areas have been extracted using the extension that we proposed in Section III-B; however, safe navigation regions are now characterized by an average occupancy probability in the interval [0, 0.45] to ensure a sufficient safety margin around obstacles without significantly reducing the workspace for navigation. Supplementary considerations about the selection of this interval can be found in [13].

Samples of path planning results using the classical A^* algorithm are presented in Figs. 9 and 10 for the two probabilistic maps that are, respectively, shown in Figs. 3(a) and 4(a). The safe travel space that is characterized by a low occupancy probability is shown in black in Figs. 9 and 10. For this application, no distinction is made between objects and the unknown space because the robot trajectory can only be planned over areas where no objects are encountered. Occupied and unknown spaces that are considered unsafe for navigation are both represented with an intermediate grayscale intensity. The path to be followed by the robot is computed with the classical A^* approach and is shown in white.

Given the distance minimization criterion that is implemented by the A^* algorithm, when the robot meets an invalid travel area along its trajectory, it might follow its borders while converging toward the goal position. Although the trajectories are not optimal in nature due to the simplicity of the path-planning algorithm that is used, these experimental results demonstrate that the enhanced LBP/C segmentation algorithm can provide a fast evaluation of the traversability of the space that ensures the safety of the robot when probabilistic occupancy maps of static environments are used. With the safe navigation areas being readily unified during the segmentation phase, the search effort for a collision-free path is reduced.

D. UAV Navigation

Another immediate extension to safe space localization for robot path planning is concerned with the navigation of UAVs, which requires target areas or potentially dangerous regions to be recognized from aerial images. Although such images considerably differ from probabilistic maps, they are also characterized by complex textures that vary according to the nature of specific regions on the ground, as perceived from a vertical and distant observation.

The proposed segmentation approach has been evaluated on aerial images extracted from Navteq [21] to estimate the potential of the proposed algorithm in a broader context. Figs. 11 and 12 present the results of segmentation, which are respectively applied on an aerial image of a quarry near the city of Vancouver and for a satellite image of the shore of Lake Ontario, both located in Canada. No modification to the segmentation parameters was required in these cases for the enhanced LBP/C segmentation method to provide convincing results as for the identification of the various areas of interest that can be used to guide an aerial vehicle at a coarse resolution.

The enhanced segmentation framework is able to identify, with precision, the key contrasting regions of a roughly uniform texture, such as the quarry in Fig. 11(b), as well as the ground and the island in Fig. 12(b). For these examples, the segmentation was set to recognize areas that are characterized by intensities within the interval [0.55, 1.0] as regions of interest for a UAV to explore. Moreover, in Figs. 11 and 12, because of the fact that the sections of the quarry, the land, and the island are not adjacent in the space, the proposed algorithm automatically identifies them as separate entities that are depicted by different colors. These experiments demonstrate the suitability of the proposed segmentation scheme for the diversity of maps and applications.

This paper, and the numerous experiments conducted in various contexts, demonstrate that the proposed enhanced segmentation technique can be directly used for applications such as path planning, collision avoidance, and interaction control for mobile or aerial robots that are navigating in unknown environments mapped by sensors with a high uncertainty level
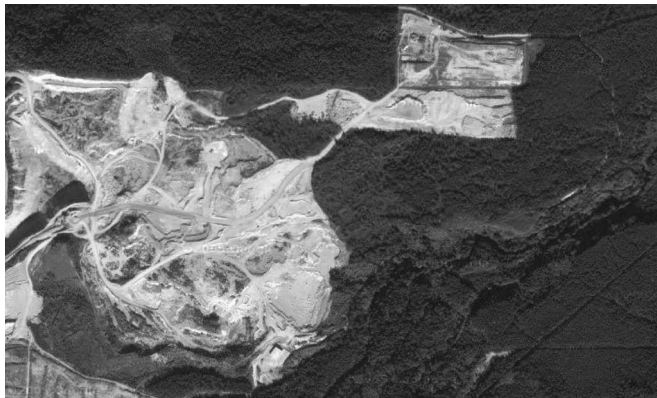
(a)
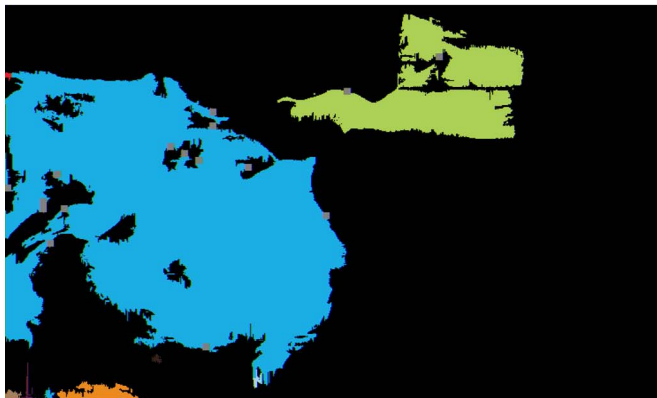
(b)

Fig. 11. Segmentation of (a) aerial image [21] of a quarry near the City of Vancouver, BC, Canada, to locate (b) disconnected segments of interest that are useful for unmanned aerial vehicle guidance.

(a)

(b)

Fig. 12. Segmentation of (a) satellite image [21] showing the land and some islands on Lake Ontario, ON, Canada, to locate (b) shoreline and disconnected segments corresponding to pieces of land.

and a limited resolution. The proposed algorithm is also computationally efficient. For example, the complete segmentation and path-planning processes for the environments that are shown in Figs. 9 and 10 take between 2 and 4 s when running on a 1.8-GHz Pentium M processor, which is realistic given the fuzzy nature of the occupancy maps with which the system is dealing.

IV. Conclusion

A revisited version of the LBP/C segmentation algorithm has been proposed and adapted to efficiently process bidimensional probabilistic occupancy maps that are encoded as textured images. Experimental results on environment maps of different nature and various complexity levels demonstrated the accuracy and the computational efficiency of the proposed approach over the original technique.

Extensions of the enhanced LBP/C algorithm have also been developed and validated. These provide greater flexibility in increasing the number of levels that are used in segment classification and in selecting the regions that are characterized by a specific range of occupancy levels. An application to safe mobile robot navigation in cluttered environments, which is strictly guided by segmented 2-D occupancy maps acquired with realistic range sensors that are submitted to a limited spatial resolution, demonstrated the relevance of the approach for collision-free robot path planning and interaction control

with the environment. The applicability of the proposed algorithm also extends beyond the processing of probabilistic maps. Indeed, it provides, without any adaptation, very satisfactory segmentation results on aerial and satellite images that can be used for UAV navigation.

Ongoing research aims at extending the proposed technique for the automatic selection of the position and the orientation of sensors during the construction of an environment map using the segmentation of a preliminary map. This will create the opportunity to evolve the framework to address the segmentation of dynamic occupancy maps. Also, a higher level of interpretation of multilevel segmented maps is under investigation to support the recognition of objects that are present in the environment from both their texture and shape, in spite of the fact that the measurements that are acquired by the sensors remain incomplete and uncertain.

References

[1] A. Elfes, "Using occupancy grids for mobile robot perception and navigation," *Comput.*, vol. 22, no. 6, pp. 46–57, Jun. 1989.
[2] X. Wu, "Adaptive split-and-merge segmentation based on piecewise least-square approximation," *IEEE Trans. Pattern Anal. Mach. Intell.*, vol. 15, no. 8, pp. 808–815, Aug. 1993.
[3] T. Hong, A. Rosenfeld, K. A. Narayanan, S. Peleg, and T. Silberberg, "Image smoothing and segmentation by multiresolution pixel linking: further experiments and extensions," *IEEE Trans. Syst., Man, Cybern.*, vol. SMC-12, no. 5, pp. 611–622, Sep./Oct. 1982.

[4] F. Arman and J. A. Pearce, "Unsupervised classification of cell images using pyramid node linking," *IEEE Trans. Biomed. Eng.*, vol. 37, no. 6, pp. 647–650, Jun. 1990.

[5] M. Spann and R. Wilson, "A quad-tree approach to image segmentation which combines statistical and spatial information," *Pattern Recognit.*, vol. 18, no. 3/4, pp. 257–269, 1985.

[6] A. K. Jain and F. Farrokhnia, "Unsupervised texture segmentation using Gabor filters," in *Proc. IEEE Int. Conf. Syst., Man Cybern.*, Los Angeles, CA, Nov. 4–7, 1990, pp. 14–19.

[7] N. Mittal, D. P. Mital, and L. C. Kap, "Features for texture segmentation using Gabor filters," in *Proc. Int. Conf. Image Process. Appl.*, Manchester, U.K., Jul. 13–15, 1999, vol. 1, pp. 353–357.

[8] D. P. Mital, "Texture segmentation using Gabor filters," in *Proc. Int. Conf. Knowledge-Based Intell. Eng. Syst. Allied Technol.*, Brighton, U.K., Aug. 30–Sep. 1, 2000, vol. 1, pp. 109–112.

[9] T. Chang and C.-C. J. Kuo, "Texture analysis and classification with tree-structured wavelet transform," *IEEE Trans. Image Process.*, vol. 2, no. 4, pp. 429–441, Oct. 1993.

[10] M. Unser, "Texture classification and segmentation using wavelet frames," *IEEE Trans. Image Process.*, vol. 4, no. 11, pp. 1549–1560, Nov. 1995.

[11] M. S. Crouse, R. D. Nowak, and R. G. Baraniuk, "Wavelet-based statistical signal processing using hidden Markov models," *IEEE Trans. Signal Process.*, vol. 46, no. 4, pp. 886–902, Apr. 1998.

[12] H. Choi and R. G. Baraniuk, "Multiscale image segmentation using wavelet-domain hidden Markov models," *IEEE Trans. Image Process.*, vol. 10, no. 9, pp. 1309–1321, Sep. 2001.

[13] B. Abou Merhy, P. Payeur, and E. M. Petriu, "Application of segmented 2D probabilistic occupancy maps for mobile robot sensing and navigation," in *Proc. IEEE Int. Instrum. Meas. Technol. Conf.*, Sorrento, Italy, Apr. 24–27, 2006, pp. 2342–2347.

[14] T. Ojala and M. Pietikäinen, "Unsupervised texture segmentation using feature distributions," *Pattern Recognit.*, vol. 32, no. 3, pp. 477–486, Mar. 1999.

[15] T. Mäenpää, T. Ojala, M. Pietikäinen, and S. Maricor, "Robust texture classification by subsets of local binary patterns," in *Proc. 15th ICPR*, Barcelona, Spain, Sep. 3–8, 2000, vol. 3, pp. 947–950.

[16] T. Ojala, M. Pietikäinen, and T. Mäenpää, "Multiresolution gray-scale and rotation invariant texture classification with local binary patterns," *IEEE Trans. Pattern Anal. Mach. Intell.*, vol. 24, no. 7, pp. 971–987, Jul. 2002.

[17] R. R. Sokal and F. J. Rohlf, *Biometry: The Principles and Practice of Statistics in Biological Research*, 2nd ed. San Francisco, CA: Freeman, 1981.

[18] T. W. Kirkman, *Statistics to Use*. Saint Joseph, MN: College Saint Benedict, Saint John's Univ., Feb. 2008. [Online]. Available: http://www.physics.csbsju.edu/stats/

[19] B. Bolzon and P. Payeur, "Experimental study of data merging techniques for workspace modeling with uncertainty," in *Proc. IEEE Int. Workshop Advanced Methods Uncertainty Estimation Meas.*, May 13, 2005, pp. 14–19.

[20] J.-C. Latombe, *Robot Motion Planning*. Boston, MA: Kluwer, 1991.

[21] Google Inc., *Navteq: Données Cartographiques*, Apr. 2006. [Online]. Available: http://maps.google.ca

Bassel Abou Merhy received the M.A.Sc. degree in electrical engineering from the University of Ottawa, Ottawa, ON, Canada, in 2006.

He is currently a Software Engineer with Nortel Networks, Ottawa. He is also with School of Information Technology and Engineering, University of Ottawa. His research interests include signal processing, image segmentation, and photonics.

Pierre Payeur (S'90–M'98) received the Ph.D. degree in electrical engineering from the Université Laval, Quebec City, QC, Canada, in 1999.

Since 1998, he has been with School of Information Technology and Engineering, University of Ottawa, ON, Canada, where he is currently an Associate Professor and the Director of Sensing and Modeling for Automation and Robotic Intelligence Research Group. He is also a founding Member of Vision, Imaging, Video, and Autonomous Systems Research Laboratory and a Member of the Sensing and Modeling Research Laboratory. He regularly serves as an external Consultant for companies in industrial automation, sensing, and robotic applications. His research interests include machine vision, motion capture, probabilistic 3-D modeling, range data processing, tactile sensing, robot guidance, and teleoperation. He has published more than 70 technical papers and supervised 40 researchers.

Dr. Payeur is a member of the IEEE Robotics and Automation Society, the IEEE Instrumentation and Measurement Society, and the Ordre des Ingénieurs du Québec. He served as the General Chair for the IEEE International Workshop on Robotics and Sensors Environments in 2007 and 2008, as well as the Technical Program Chair and a Committee Member for more than 35 international conferences on instrumentation and measurement, computer vision, and robotics. He also regularly serves as a reviewer for several journals and transactions in the same fields.

Emil M. Petriu (M'86–SM'88–F'01) received the Dipl. Eng. and Dr. Eng. degrees from the Polytechnic Institute of Timisoara, Timisoara, Romania, in 1969 and 1978, respectively.

Since 1985, he has been a member of the faculty of the University of Ottawa, Ottawa, ON, Canada, where he is currently a Professor and the University Research Chair with School of Information Technology and Engineering. Since 2005, he has been serving as the Chief Scientific Officer of XYZ RGB Inc., Ottawa, which is a 3-D imaging company. He has published more than 280 technical papers, authored two books, and edited other two books. He is the holder of two patents. His research interests include robot sensing and perception, interactive virtual environments, human–computer symbiosis, soft computing, and digital integrated circuit testing.

Dr. Petriu is a Fellow of the Canadian Academy of Engineering and of the Engineering Institute of Canada. He is currently serving as the Chair of TC-15 Virtual Systems and a Cochair of TC-28 Instrumentation and Measurement for Robotics and Automation and TC-30 Security and Contraband Detection of the IEEE Instrumentation and Measurement Society. He was the General Chair of the IEEE Instrumentation and Measurement Technology Conference (IMTC), May 2005, Ottawa, and will be chairing the IEEE International Conference on Virtual Environments, Human–Computer Interfaces and Measurement Systems (VECIMS), July 2008, Istanbul, Turkey. He was also the Program Chair of IMTC 1997, Ottawa; IMTC 1998, St. Paul, MN; IMTC 2002, Anchorage, AK; I^2MTC 2008, Victoria, BC, Canada; the IEEE International Workshop on Measurement Systems for Homeland Security (IMS), Contraband Detection and Personal Safety, March 2005, Orlando, FL; IMS 2006, Alexandria, VA; and VECIMS, June 2007, Ostuni, Italy. He is an Associate Editor of the IEEE TRANSACTIONS ON INSTRUMENTATION AND MEASUREMENT and a member of the editorial board of the *IEEE Instrumentation and Measurement Magazine*. He was a corecipient of the IEEE's Donald G. Fink Prize Paper Award and the recipient of the IEEE Instrumentation and Measurement Society Award in 2003.